AIAA JOURNAL
Vol. 36, No. 6, June 1998

Wave Number Frequency Spectra of a Lifting Wake for Broadband Noise Prediction

William J. Devenport* and Christian W. Wenger†
Virginia Polytechnic Institute and State University, Blacksburg, Virginia 24061
Stewart A. L. Glegg‡
Florida Atlantic University, Boca Raton, Florida 33431
and
Joseph A. Miranda§
U.S. Naval Undersea Warfare Center, Newport, Rhode Island 02841

Measurements of wave number frequency spectra of velocity fluctuations have been made using two three-component hot-wire probes in the wake of a rectangular NACA 0012 half-wing at a 5-deg angle of attack. Spectra were measured along spanwise lines in the near two-dimensional part of the wake, in the stretched region where the wake begins to wind around the vortex, directly above the vortex core, and radially from the core center. Dominated by the large-scale organized motions present in the wake, the spectra show little similarity with the von Kármán isotropic turbulence spectrum. Outside the core, upwash spectra contain a single maximum at the passage frequency of these large structures. Motions associated with this peak are highly anisotropic, both in terms of velocity components and length scales. Similar anisotropy is also seen at higher wave numbers, suggesting either that the smaller scale turbulent motions are organized by the large eddies or that the nonsinusoidal components of those eddies contribute significantly to the spectrum at higher wave numbers. The implications of these results for broadband noise prediction have been assessed by considering the sound radiation from this turbulent flow over a semi-infinite flat plate. The major conclusion is that the correlation length scales of the flow are small compared to the acoustic wavelength and so are well represented by their values at zero spanwise wave number. However, the blade response function has a variation with spanwise wave number that cannot be ignored and significantly influences the spanwise directionality.

Nomenclature

c	= chordlength of wing, 8 in. (203 mm)
c_0	= speed of sound
d	= half-span of the noise generating blade [Eq. (8)]
G_{ww}	= cross-spectral density [Eq. (1)]
K_x	= nominal streamwise wave number, ω/U_∞
k_e	= reference wave number $\sqrt{\pi}\,\Gamma(\frac{5}{6})/\Gamma(\frac{1}{3})/L$
k_y	= spanwise wave number
L	= reference/integral length scale
$\mathcal{L}$	= blade response function [Eq. (12)]
L_{wake}	= wake half-width
$l(\omega)$	= spanwise upwash length scale [Eq. (6)]
M	= Mach number
U_∞	= freestream velocity
u, v, w	= velocity components along x, y, z
x, y, z	= coordinates defined in Fig. 1
y'	= probe separation in the y direction
β	= $\sqrt{(1-M^2)}$
γ	= $\omega(M - x/\sigma)/c_0\beta^2$
θ	= observer angle, $\arcsin(y\beta/\sigma)$
κ	= $K_x M/\beta^2$
κ_e	= $\kappa^2 - k_y^2/\beta^2$
ρ_0	= density
σ	= $\sqrt{[x^2 + \beta^2(y^2+z^2)]}$
Φ_{ww}	= full wave number frequency spectrum [Eq. (3)]
ϕ_{ww}	= pointwise wave number frequency spectrum [Eq. (2)]
ω	= angular frequency

Received March 19, 1997; presented as Paper 97-1699 at the AIAA/CEAS 3rd Aeroacoustics Conference, Atlanta, GA, May 12–14, 1997; revision received Nov. 25, 1997; accepted for publication Jan. 20, 1998.

*Associate Professor, Department of Aerospace and Ocean Engineering. Senior Member AIAA.
†Undergraduate Researcher, Department of Aerospace and Ocean Engineering. Student Member AIAA.
‡Professor, Department of Ocean Engineering. Senior Member AIAA.
§Mechanical Engineer, Solid Mechanics and Design Branch. Member AIAA.

I. Introduction

BROADBAND noise is generated when an airfoil passes through turbulence. To predict the radiated noise it is necessary to model the interaction of the turbulent flow with the body. This difficult problem is usually solved by linearizing the governing equations and then examining the response of the foil to an infinitely extending sinusoidal upwash gust. The response to the full turbulent flow is then obtained as a linear sum of sinusoids over the wave number frequency spectrum of the turbulence, this representing the distribution of spanwise length scales as a function of frequency seen by the leading edge as it cuts the turbulent flow.

One of the problems with this approach is that there are no established methods for predicting the wave number frequency spectrum of turbulent flows. Most experimental and theoretical studies of this descriptor have dealt exclusively with homogeneous isotropic turbulence. Out of necessity, therefore, broadband noise predictions usually assume a homogeneous isotropic turbulence type spectrum, e.g., von Kármán, even though it is rare for the turbulent flow producing the noise to fit either of these forms.

Our purpose is to examine the implications and accuracy of this necessary but drastic assumption. To do this we present measurements of wave number frequency spectra in a representative turbulent flow, compare these with a von Kármán spectrum, and then assess the implications that the differences have for broadband noise prediction.

II. Flow

As the representative flow we choose the wake of a lifting rectangular wing. In many applications broadband noise is generated by interactions between airfoils and wake type flows. A lifting wake contains many of the features, both simple and complex, often found in such flows.

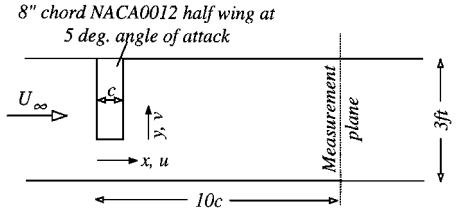

Fig. 1 Schematic of the wind-tunnel test section showing the coordinate system; coordinate z and corresponding upwash velocity component w are directed out of the paper so as to complete a right-handed system.

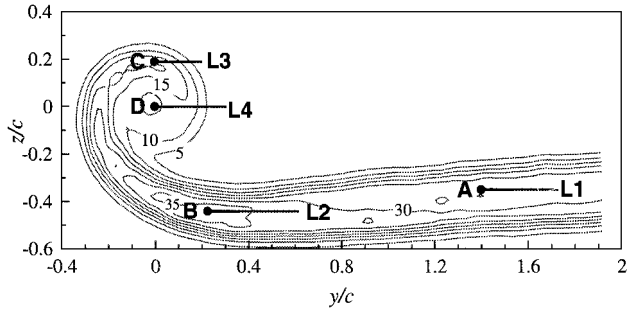

Fig. 2 Contours of axial turbulence normal stress $\bar{u}^2/U_\infty^2 \times 10^5$ measured 10 chordlengths downstream of the wing leading edge and two-point measurement locations: points A–D locations of fixed probe and adjoining lines L1–L4 traverse directions for movable probe.

The flow, documented and discussed in detail by Miranda and Devenport,[1,2] was generated in the $3 \times 2 \times 20$ ft^3 test section of the Virginia Tech Subsonic Wind Tunnel using a rectangular planform, NACA 0012 half-wing (aspect ratio 6) at an angle of attack of 5 deg and Reynolds number 3.2×10^5 (based on the 0.203-m chord c) (Fig. 1). The wing was mounted at the midheight of the test section and extended two-thirds of the distance across its 3-ft width. Boundary layers on both sides of the wing were tripped to avoid instability associated with transition and to increase the Reynolds number of the axial wake. Detailed three-component velocity and turbulence measurements were made using a four-sensor, hot-wire probe over the wake cross section $10c$ downstream of the leading edge.

Figure 2 shows the overall flow structure at this station in terms of contours of axial turbulence normal stress normalized on the approach freestream velocity U_∞. Coordinates y and z that define positions in this crossflow plane have their origins at the vortex center. The wake consists of a small concentrated vortex core, of radius 3.9%c, surrounded by a circulating velocity field that winds the wing wake into an ever increasing spiral. Far from the vortex core ($y/c > 1$), the flow is similar to an equilibrium two-dimensional wake and nearly homogeneous in the spanwise y direction. Mean velocity and turbulence stress profiles through this part of the wake resemble those measured by Wygnanski et al.,[3] Townsend,[4] Antonia and Britz,[5] and others in equilibrium two-dimensional turbulent wakes. The half-thickness of the wake here (defined as the distance from the wake center to the point where the mean axial velocity deficit is half its centerline value) is $0.083c$. Autospectra of upwash w velocity fluctuations (Fig. 3) measured near the wake centerline in this region have a form much like those presented by Antonia and Britz.[5] Among other features, they display a peak at a nondimensional frequency $K_x c = \omega c/U_\infty$ of about 20 presumably generated by the passage of the predominantly spanwise-oriented eddies that one expects to dominate the instantaneous flowfield.

Moving outboard (in the negative y direction), the wake comes under the influence of the mean flowfield of the vortex, subjecting it to increasing lateral stretching, curvature, and skewing. These influences are documented quantitatively by Miranda and Devenport.[1,2] The dominant effect is lateral stretching. Consistent with earlier studies, such as that of Keffer,[6] stretching thins the wake and appears to organize and intensify the dominant spanwise eddies. This leads to some increase in axial turbulence levels to a maximum near $y/c = 0.2$, $z/c = -0.4$ and an enhancing of the coherent-structure peak seen in the w autospectrum (Fig. 3). Moving farther along the

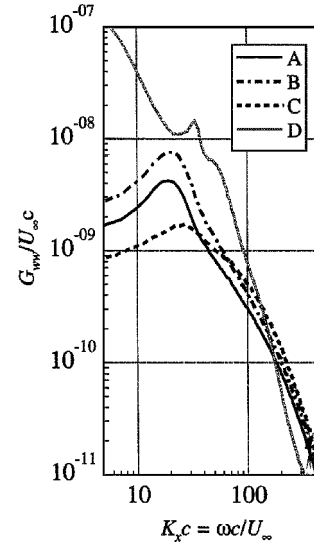

Fig. 3 Autospectra of upwash velocity fluctuations at locations A–D; see Fig. 2.

spiral wake, turbulence levels start to fall as the wake continues to thin and weaken. Although it is not apparent in Fig. 1, this drop in turbulence levels continues as the core is entered. The increase in turbulence levels seen in the core region in Fig. 2 is actually produced by vortex wandering the slow side-to-side motion of the vortex that causes the high-velocity gradients in the core to appear as large turbulence levels. Using techniques developed by Devenport et al.,[7] Miranda and Devenport[1,2] estimated the rms vortex wandering amplitude about 0.35%c. The true turbulence structure in the core center is to some extent visible in velocity autospectra measured there (location D, Fig. 3). Compared with spectra measured in the spiral wake (locations A, B, or C), these show very high spectral levels at low frequencies $K_x c < 20$ associated with wandering but much lower levels at high frequencies $K_x c > 200$, indicating that the core may be devoid of smaller turbulence scales and perhaps may be laminar. Devenport et al.[7] show via several other methods that this is, indeed, the case. One interesting feature of the spectra is that they show substantial energy in core-center velocity fluctuations in the midfrequency range $20 < K_x c < 200$. Devenport et al.[7] hypothesized that this was inactive motion (including, perhaps, core waves) produced as the core was buffeted by the surrounding wake turbulence.

Miranda and Devenport[1,2] presented many other results, not least a detailed sequence of velocity and turbulence profiles perpendicular to the spiral-wake centerline. Our central focus here, however, is on two-point measurements made in this flow and implications of those measurements for broadband noise prediction. The two-point measurement locations are shown in Fig. 2.

III. Two-Point Hot-Wire Anemometry

Measurements were made using two Auspex Corporation miniature four-sensor hot-wire probe, type AVOP-4-100. This type of probe, consisting of two orthogonal X-wire arrays, was chosen because it is capable of simultaneous three-component measurements from a relatively compact (0.5 mm^3) measurement volume. It also overcomes some of the gradient error problems associated with a standard triple-wire probe in trailing vortex flows.[8,9] Sensors were operated using Dantec 56C17/56C01 anemometer units (matched frequency response better than 20 kHz) interfaced to an IBM AT compatible computer using an Analogic 12-bit HSDAS-12 analog-to-digital converter and a series of buck and gain amplifiers of calibrated frequency response.

Probes were calibrated separately for velocity and angle response. Velocity calibrations were performed frequently in the freestream using King's law to correlate the wire output voltages with the cooling velocities. Angle calibrations were performed periodically using the direct method of Devenport et al.[7] and Wittmer et al.,[9] which involves placing the probe in the potential core of a uniform jet and pitching and yawing over all likely flow angle combinations from +45 to −45 deg.

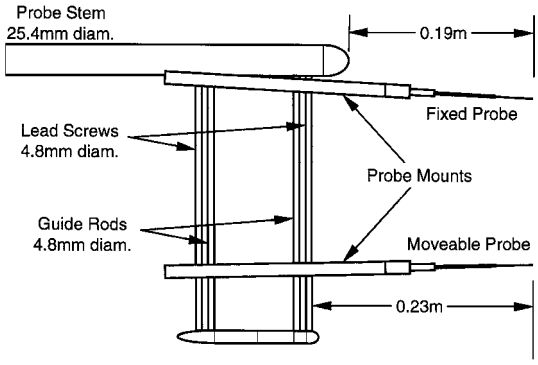

Fig. 4 Probe holder used for two-point measurements; note angling of probe mounts to reduce minimum separation.

Two-point measurements were performed using the specially constructed probe holder shown in Fig. 4. This holder includes a computer controlled traverse used to adjust the spanwise separation of the two probes. The holder was mounted in the two-axis wind-tunnel traverse so that the y and z locations of both probes could be adjusted independent of their separation.

Extensive probe interference studies using the two-probe support were performed by Miranda.[10] The support and probes were placed at various locations around and within the vortex while helium filled soap bubbles were used to visualize the center of the vortex core. The core and the flow surrounding it appeared completely undisturbed by the probes and the holder at the measurement point. Miranda[10] also made velocity measurements to examine interference. He did find an effect but it was small, producing at most a 0.7% change in the measured mean velocity for the smallest probe separation. The approximate magnitude of this effect was predicted by Devenport et al.[7] using a potential flow model of a single probe.

IV. Data Acquisition and Analysis

Four sequences of two-point measurements were made on four spanwise (y direction) lines through the flow to reveal the flow as it would be seen by a hypothetical blade cutting the wake (Fig. 2). Data were taken in the near two-dimensional portion of the wake (point A, line L1, Fig. 2); the stretched part of the wake, around the maximum in turbulence levels (point B, line L2, Fig. 2); the highly curved and strained portion of the wake found above the core (point C, line L3, Fig. 2); and radially from the core center itself (point D, line L4, Fig. 2). For each sequence of measurements one of the probes was held at a fixed point (points A–D) while the other probe was traversed to a number of locations along the intersecting horizontal line (lines L1–L4). At each probe separation, 100 3072-point records were recorded for each of the eight simultaneous sensor signals at a sampling frequency of 50 kHz and over a total measurement time of some 2 min.

By angling the probes toward each other (by about 2 deg each) in the probe holder (Fig. 4), it was possible to make measurements with the center points of the two-probe measurement volumes separated by only 3 mm ($0.0158c$). (The instantaneous velocity vectors measured by the probes were, of course, rotated back during processing to account for this misalignment.) A very small minimum separation is desirable when making two-point measurements because it enables one to fully define the cross spectrum as a function of separation even at high frequencies. Separations of the present probes of less than 3 mm were considered too risky, however, and, given the 0.8-mm diameter of their measurement volumes, unlikely to produce meaningful results. Furthermore, as will be discussed, the minimum probe separation was not found to be a limiting factor in determining wave number frequency spectra. Measurements were made typically to a maximum probe separation of about 65 mm at a total of about 70 separations.

Measurements were first processed by taking the fast Fourier transform (FFT) of the velocity time-series signals and using them to compute the cross spectrum between the fixed and traversing probes as a function of probe separation y', e.g.,

$$G_{ww}(y, y', \omega) = \lim_{T\to\infty} (\pi/T) E[w^*(y, \omega) w(y + y', \omega)] \qquad (1)$$

where y denotes the spanwise location of the fixed probe (x and z being implicit) and similar expressions for u and v. Note that the coordinates and components used here are defined in Fig. 1. Typically 150 realizations of the 1024-point FFTs were averaged to form the expected value, sufficient to produce a smooth, low-uncertainty spectrum.

These cross-spectral functions were then further processed by Fourier transforming them with respect to y'. The result is a pointwise wave number frequency spectrum about the fixed probe location y:

$$\phi_{ww}(K_x, k_y, y) = \frac{U_\infty}{2\pi} \int_{-\infty}^{\infty} G_{ww}(y, y', \omega)\, e^{-jk_y y'}\, \mathrm{d}y' \qquad (2)$$

where $K_x = \omega/U_\infty$. Note that, because measurements were made only for positive separations y', it was necessary to assume symmetry of the cross spectrum, i.e., even real part and odd imaginary part, with y' to perform this transform. As a result the calculated ϕ_{ww} were entirely real.

It is important to realize that in some situations this pointwise spectrum differs from the full wave number frequency spectrum used to characterize homogeneous turbulent flows in broadband noise prediction schemes, e.g., Ref. 11. A rigorous definition of this spectrum is the double Fourier transform of the space–time velocity autocorrelation function, i.e.,

$$\Phi_{ww}(K_x, k_y) = \frac{U_\infty}{4\pi^2} \int_{-\infty}^{\infty}\int_{-\infty}^{\infty} \lim_{T\to\infty} \frac{1}{RT} \int_{-T/2}^{T/2}\int_{-R/2}^{R/2} w(y, t) \times w(y + y', t + \tau)\, \mathrm{d}y\, \mathrm{d}t\, e^{-j\omega\tau} e^{-jk_y y'}\, \mathrm{d}\tau\, \mathrm{d}y' \qquad (3)$$

which may be rewritten in terms of the two-point cross spectrum $G_{ww}(y, y', \omega)$ as

$$\Phi_{ww}(K_x, k_y) = \frac{U_\infty}{2\pi R} \int_{-\infty}^{\infty}\int_{-R/2}^{R/2} G_{ww}(y, y', \omega)\, \mathrm{d}y\, e^{-jk_y y'}\, \mathrm{d}y' \qquad (4)$$

and, thus, we see that

$$\Phi_{ww}(K_x, k_y) = \frac{1}{R} \int_{-R/2}^{R/2} \phi_{ww}(K_x, k_y, y)\, \mathrm{d}y \qquad (5)$$

That is, the traditional wave number frequency spectrum is the spanwise average of the pointwise spectrum used here. This distinction between ϕ_{ww} and Φ_{ww} disappears when the flow is independent of y, such as is almost the case along lines L1 and L2 in the present flow (Fig. 2). However, in the inhomogeneous turbulent flow along lines L3 and L4, ϕ_{ww} would have been a strong function of the fixed-probe location y and the averaging that has not been performed should be borne in mind when interpreting results.

The Fourier transform in Eq. (2) was also performed by FFT. To apply the FFT algorithm it was necessary to linearly interpolate the data to equal intervals in y' and zero pad it to give a number of intervals equal to an integer power of 2 (in this case 128). At all separations except the smallest, the resolution and range in y' before interpolation was easily sufficient to capture the shape of G_{ww} (or G_{uu} or G_{vv}) and its complete decay to zero at larger separations. The smallest separation ($0.0158c$), however, was too large to resolve the variation in the cross spectra at small y' for higher frequencies, this function becoming more and more like a delta function in y' with increase in frequency. To examine the effects of this underresolution, the linear interpolation at small y' was replaced with a smooth interpolation based on the Liepmann isotropic turbulence spectrum.[11] This produced no discernible effect on the final wave number frequency spectrum, at least over the frequency and wave number ranges of interest here. This result was both surprising and welcome because we expected the minimum probe separation to pose a much more serious limit on the measured wave number frequency spectra.

V. Wave Number Frequency Spectra

Figures 5 and 6 show the real wave number frequency spectra calculated from the measurements made on lines L1–L4 about points

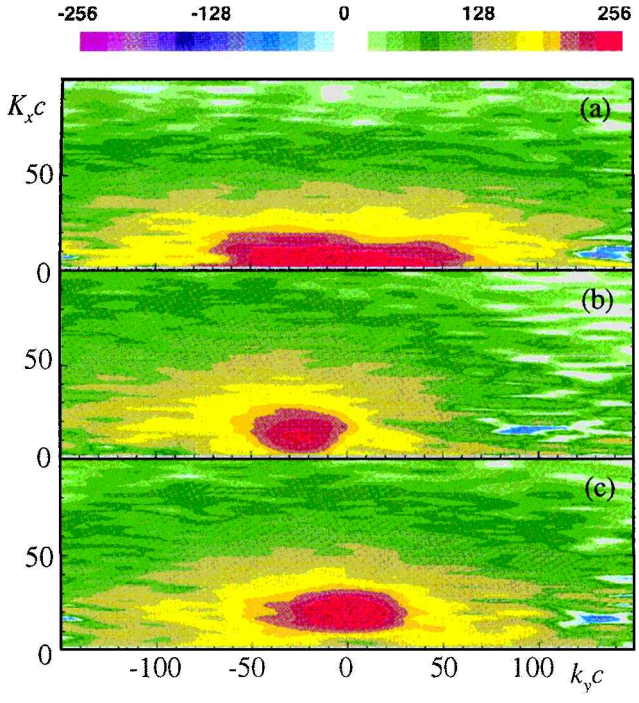

Fig. 5 Wave number frequency spectra at location A/L1 $\times 10^6$: a) $\phi_{uu}/\bar{u}^2c^2$, b) $\phi_{vv}/\bar{v}^2c^2$, and c) $\phi_{ww}/\bar{w}^2c^2$.

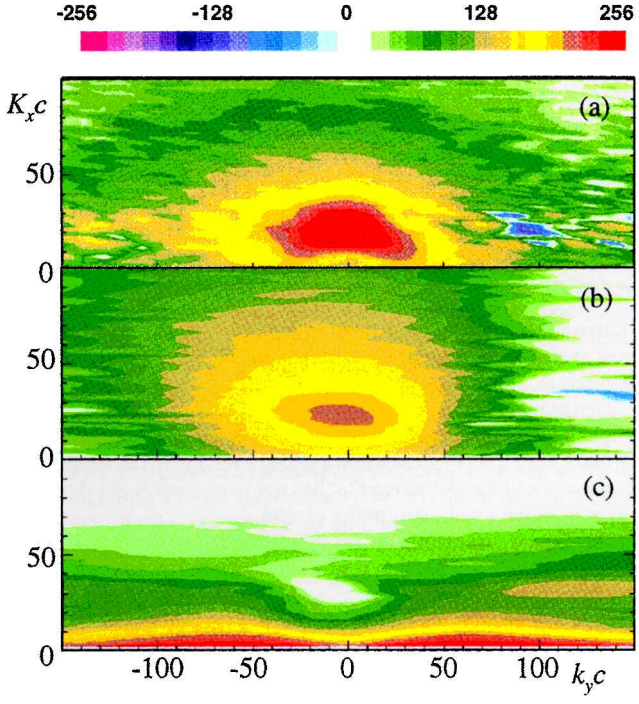

Fig. 6 Upwash w wave number frequency spectra $\phi_{ww}/\bar{w}^2c^2 \times 10^6$ at locations a) B/L2, b) C/L3, and c) D/L4.

A–D respectively. Most interesting from the point of view of broadband noise prediction is the upwash w components of these spectra. In the case of L1, however, we also present u- and v-component spectra because they reveal, by comparison, some of the anisotropy of the turbulence as well as further information about its structure. The spectra are plotted vs normalized spanwise wave number k_yc and frequency expressed as the nominal streamwise wave number $K_xc = \omega c/U_\infty$. In all plots spectral levels have been normalized on the mean square fluctuation of the relevant velocity component at the fixed probe location. This ensures that all of the spectra integrate to unity.

We begin our discussion with the spectra of Fig. 5, measured on the centerline of the near two-dimensional part of the wake at location A/L1. It is well known that the far wakes of two-dimensional bodies are dominated by large-scale quasiperiodic eddies. Inevitably these eddies carry the same spanwise vorticity seen in the mean flowfield and, thus, have a preferred orientation in the spanwise direction. It is also known (see, for example, Ref. 12) that these eddies tend to have smaller spanwise than streamwise extent. All these features are visible in Fig. 5. The upwash spectrum (Fig. 5c) shows a strong peak centered on the K_x axis at $K_xc = 20$, the same frequency as the peak in the w autospectrum at point A (Fig. 3), presumed to be the passage frequency of large eddies. The frequency $K_xc = 20$ implies a structure spacing of about $0.3c$, which seems reasonable given the width of the wake at this location (Fig. 2). Surrounding this peak the spectrum decays away in all directions. Both the peak and the decay appear stretched, by a factor of 2–3 in the spanwise direction, indicative of a spanwise correlation length scale one-half to one-third of that in the streamwise direction. It is particularly interesting that this difference in scales continues to be apparent at higher wave numbers. It suggests either that the smaller scale turbulent motions tend to be organized by the anisotropy of the large eddies or that the nonsinusoidal components of those eddies contribute substantially to the spectrum at higher wave numbers.

Anisotropy in the turbulence structure is also seen when the spectra for different components are compared. Unlike the upwash component, the axial component (Fig. 5a) reaches its peak values in a strip along the k_y axis. The peak in the spanwise v component (Fig. 5b) is much weaker than that in w and is displaced to a negative k_yc of about 25. This implies that there is a phase lag between v velocity fluctuations at location A and those at points along L1. Such a phase lag could be produced by skewing of the coherent structures with respect to the y direction, but in that case one would expect to see the same asymmetry in the upwash spectrum. A more probable explanation is that the distribution of spanwise flow along the axes of the coherent structures is particularly sensitive to spanwise nonuniformity and is here biased by the influence of the distant vortex.

Anisotropy in the velocity components and length scales and quasiperiodicity in velocity fluctuations are fairly common features of the larger coherent motions that dominate most turbulent flows, particularly wakes. They are all, of course, absent in homogeneous turbulence. It is, therefore, hardly surprising that these spectra bear little resemblance to the highly idealized form of the von Kármán spectrum (Fig. 7). The semicircular contours of the von Kármán spectrum simply do not represent the spectral features produced by the coherent structure of the turbulence or account for the accompanying anisotropy of the smaller turbulence scales.

Figure 6a shows the upwash spectrum computed about point B using measurements along L2 (Fig. 2). At location B the wake is beginning to be significantly influenced by the vortex velocity field, which stretches it in the spanwise direction. Stretching should intensify and better organize the dominant spanwise eddies, as well as increasing their spanwise scale.[6] Consistent with this, the spectrum shows an increase in the intensity of the peak associated with the eddies (at $K_xc = 20$, $k_yc = 0$) and some change in the shape of the contours that define it and the surrounding decay. Even at higher wave numbers the contours are noticeably less elliptical in appearance suggesting an increase in the spanwise scale of the turbulence compared to the streamwise scale.

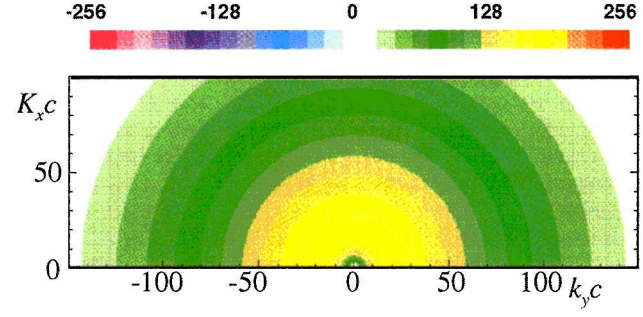

Fig. 7 Von Kármán spectrum plotted in terms of K_xc and k_yc by using an integral length scale $L = 0.03c$.

Figure 6b shows the upwash spectrum for point C/line L3, where the influence of the vortex on the wake is very strong. The radius of curvature of the wake here is comparable to its thickness, and the rates of stretching and skewing it suffers in the tangential velocity field of the vortex are of the same order as the peak axial velocity gradients within it.[1] Despite these influences the wave number frequency spectrum still shows the same coherent-structure peak near $K_x c = 20$, $k_y c = 0$. This peak is also still visible in the single-point spectrum (Fig. 3). In both representations, however, the peak is substantially weakened, perhaps indicating some reduction in the proportion of the energy in the coherent motions. Moving away from the peak, the decay of the spectrum with increase in frequency appears much more gradual than at location A or B. The decay with increase in k_y occurs at about the same rate, however, resulting in a much more isotropic spectrum. It is as though the highly anisotropic stretching, skewing, and curvature experienced at this location act to break up the larger scale organized motions releasing their influence over the smaller turbulence scales and, paradoxically, producing a more isotropic turbulent flow. Although the decay of the spectrum is more isotropic, it is still quite unlike the von Kármán spectrum of Fig. 7, primarily because it is centered on or near the coherent structure peak, rather than about the origin. (Although much less clear, a similar effect may be visible in the spectra measured at locations A and B.) A shift in the origin of a spectrum is equivalent to a modulation in the time–space domain. It is as though the velocity fluctuations associated with the smaller structures are modulated by the dominant large-scale eddies, an inevitable result if one believes that the small-scale turbulence is not uniformly distributed throughout the large eddy structure.

Figure 6c, the upwash wave number spectrum measured about the vortex core center at location D, bears little if any resemblance to spectra measured in the spiral wake. The spectral contours are almost parallel to the k_y axis, with most of the energy in the spectrum being concentrated in a ridge that runs along that axis. The implication is that velocity fluctuations in and around the core are concentrated in very low-frequency motions of small spanwise extent. These motions are, of course, the vortex wandering. Interestingly, wandering is not the only feature seen in the spectrum. The depression centered on the K_x axis occurs at the same frequency ($K_x c = 35$) as the sharp peak visible in the core center autospectrum (Fig. 3). We suspect that both are the result of core motions stimulated as the core is buffeted by the turbulence that surrounds it.

VI. Length Scales

In Amiet's[11] approximation, the influence of the wave number frequency spectrum on the far-field noise may be represented in terms of the spanwise correlation length scale spectrum

$$l(\omega) = \frac{1}{G_{ww}(y, 0, \omega)} \int_0^\infty G_{ww}(y, y', \omega)\, \mathrm{d}y'$$

$$= \frac{\pi}{U_\infty} \phi_{ww}(y, 0, \omega)/G_{ww}(y, 0, \omega) \tag{6}$$

The present measurements were used to compute $l(\omega)$ at the three locations A, B, and C in the spiral wake. As indicated, the length scale can be determined either from the wave number frequency spectrum or by integration of the cross spectrum as a function of separation y'. Both methods applied to the present data produced identical results.

Results are plotted in Fig. 8, where they are compared with the length scale spectrum implied by the von Kármán isotropic turbulence spectrum. This comparison is made by normalizing $l(\omega)$ on the length scale L, taken here to be the local half-width of the wake

Table 1 Comparison of various measures of the integral length scale at locations A/L1–D/L4 with the wake half-width L_{wake}

Point	A	B	C	D
$L_{u,x}$	10.6	7.7	5.5	7.3
$L_{w,x}$	2.8	2.7	2.0	33.0
$L_{u,y}$	6.1	8.5	4.0	0.1
$L_{w,y}$	9.8	15.0	7.9	−6.8
L_{wake}	16.9	12.2	6.7	——

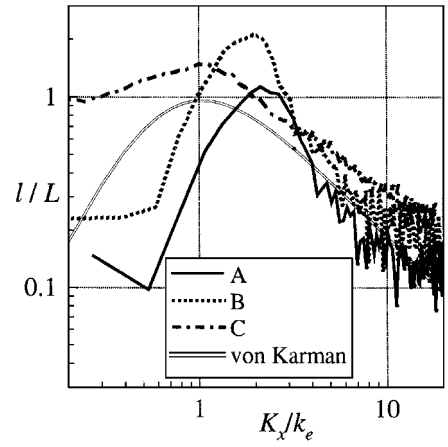

Fig. 8 Length scale spectra about locations A–C and inferred from the von Kármán spectrum.

L_{wake} listed in Table 1 (length scales in millimeters, 203.2-mm wing chord) and by normalizing frequency $K_x (= \omega/U_\infty)$ on the corresponding reference wave number $k_e = [\Gamma(\frac{5}{6})/\Gamma(\frac{1}{3})]\sqrt{\pi}/L$. For the von Kármán spectrum, L is the streamwise integral length scale of the streamwise velocity fluctuations $L_{u,x}$

$$L_{u,x} = \int_0^\infty R_{uu}(x)\, \mathrm{d}x \tag{7}$$

where R_{uu} is the autocorrelation coefficient function.

Despite the large differences between the von Kármán and measured wave number frequency spectra, the length scale spectra in Fig. 8 do show some similarity. At higher frequencies ($K_x/k_e > 4$) all of the measured spectra show roughly the same decay rate as the von Kármán spectrum, having a -1 slope on this log-log scale. At lower frequencies, however, the influence of the quasiperiodic large-scale eddies dominates the length scale, producing much more pronounced peaks than are apparent in the von Kármán spectrum.

Some of the quantitative differences between the length scale spectra may be attributed to the normalization. It would be nice to be able to use a length scale for the wake spectra that would be precisely equivalent to the integral scale used with the isotropic turbulence spectrum. However, the anisotropy of the wake turbulence and the organized large-scale structure that dominate it make it almost impossible to define such a scale. To illustrate this point, we have computed, and present in Table 1, integral length scales for the four measurement locations A–D. We present the integral length scale of the streamwise velocity fluctuations $L_{u,x}$ and the analogously defined streamwise and spanwise integral length scales of the upwash and streamwise components $L_{w,x}$, $L_{w,y}$, and $L_{u,y}$. The streamwise x correlation functions and integrations needed for $L_{w,x}$ and $L_{u,x}$ were performed assuming Taylor's hypothesis.

The different length scale estimates vary widely. It is particularly noticeable that at the points in the spiral wake (A, B, C) the streamwise length scale of the upwash component $L_{w,x}$ is consistently much smaller than the spanwise length scale of this component $L_{w,y}$. This appears in contradiction to the wave number frequency spectra, which clearly indicate a smaller spanwise than streamwise length scale. The misleading length scales arise because the $R_{ww}(x)$ functions contain large negative excursions (directly associated with the quasiperiodicity in the large eddies) that reduce the corresponding length scale, whereas $R_{ww}(y)$ remains entirely positive. One could, therefore, argue that $L_{w,y}$ is an appropriate length scale and, indeed, it does show some physically meaningful variation (growing as the wake becomes laterally stretched between locations A and B). However, such a measure would be no more appropriate than, for example, the more easily determined wake width, which we have preferred to use in this case.

The variability of integral length scales in anisotropic flows is seen in its most extreme for location D, in the core center. Here the streamwise integral length scale of the upwash component becomes extremely large because of the wandering. The same motion produces such large negative regions in the spanwise autocorrelation function that the resulting spanwise length scale is negative.

VII. Implications for Sound Radiation from an Airfoil

We will consider the implications of these results to the sound radiation from an airfoil in a turbulent stream. Specifically, we use the results measured at locations A/L1 and B/L2. Because the wake was locally homogeneous in the spanwise direction at these locations, the measured pointwise wave number frequency spectra provide direct estimates of the full wave number frequency spectra that would be used as part of a broadband noise prediction. We base our analysis on the formulation given by Amiet,[11] who considered sound radiation from an airfoil in a homogeneous turbulent flow using a von Kármán spectrum. We will compare predictions of the acoustic field obtained using this theoretical spectrum with those which would be obtained using the measurements described in the preceding sections.

Amiet[11] gives the spectral density of the sound pressure in the far field of an airfoil with large span as

$$S_{pp}(x, y, z, \omega) = \left(\frac{\omega z \rho_0}{c_0 \sigma}\right)^2 \pi U_\infty d \left|\mathcal{L}\left(x, K_x, \frac{\omega y}{c_0 \sigma}\right)\right|^2 \times \Phi_{ww}\left(K_x, \frac{\omega y}{c_0 \sigma}\right) \tag{8}$$

where x, y, z identify the observer position (using the same coordinate system as that in Fig. 1, except with an origin at the leading edge of the hypothetical noise-generating airfoil) and c_0 and ρ_0 the freestream sound speed and density. $\Phi_{ww}(K_x, k_y)$ is defined from the cross spectrum of the upwash velocity fluctuations as

$$\Phi_{ww}(K_x, k_y) = \frac{U_\infty}{2\pi} \int_{-\infty}^{\infty} G_{ww}(y, y', \omega)\, e^{-jk_y y'}\, \mathrm{d}y' \tag{9}$$

which is the same as Eq. (2), but with the implicit assumption of homogeneous turbulence. The function $\mathcal{L}$ is defined as the Fourier transform of the blade surface pressure ΔP in response to a harmonic upwash gust of the type $w_0 \exp[i K_x (x - U_\infty t) - i k_y y]$ defined as

$$\mathcal{L}(x, K_x, k_y) = \int_0^c \frac{\Delta P(x', k_y)}{2\pi \rho_0 U_\infty w_0} \exp\left[i\omega x'(M - x/\sigma)\big/ c_0 \beta^2\right] \mathrm{d}x' \tag{10}$$

An important feature that is included here is the dependence of the far-field sound on the spanwise wave number k_y.

To simplify his result, Amiet[11] also considered the case when the cross spectrum in Eq. (9) decayed sufficiently rapidly that the exponential term in the integrand could be ignored for the values of k_y needed in Eq. (8), i.e., so that $\Phi_{ww}(K_x, k_y)$ could be replaced by $\Phi_{ww}(K_x, 0)$ expressed in terms of the length scale spectrum $l(\omega)$ defined in Eq. (6). Because the maximum value of k_y needed in Eq. (8) is roughly equal to K_x, we may examine Amiet's[11] approximation by comparing $\Phi_{ww}(K_x, 0)$ and $\Phi_{ww}(K_x, K_x)$, as is done in Fig. 9. This comparison shows some differences, in particular a shift in the spectral peak between $\Phi_{ww}(K_x, 0)$ and $\Phi_{ww}(K_x, K_x)$. For the measured spectra the peak shifts to lower frequencies and is reduced by ~4 dB. The von Kármán spectrum shows a smaller reduction in the peak frequency and not as large a drop in level. To assess the implications of these differences on the far-field sound radiation, we need to evaluate Eq. (8) with the correct dependence of the blade response function on spanwise wave number, as is done subsequently.

Figure 9 also provides a comparison of the measured and the von Kármán spectra as they would be used in a noise computation. It reveals large differences between the theoretical and measured spectra at lower frequencies. Because differences in the shape of Φ_{ww} will lead to similar differences in S_{pp} we conclude that, in the context of noise prediction, the von Kármán model does not adequately represent the turbulence spectrum of the present wake flows.

To incorporate the dependence of the blade response function on spanwise wave number, we idealize the blade as a semi-infinite flat plate, allowing the response function to be written in a simple algebraic form. We write

$$\Delta P(x', k_y) = \int_{-\infty}^{\infty} \frac{-i\rho_0 w_0 U_\infty e^{-i\gamma x'}}{\pi \beta (\kappa_e + \kappa M + K_x)^{\frac{1}{2}} (\kappa_e - \kappa M + \gamma)^{\frac{1}{2}}} \mathrm{d}\gamma \tag{11}$$

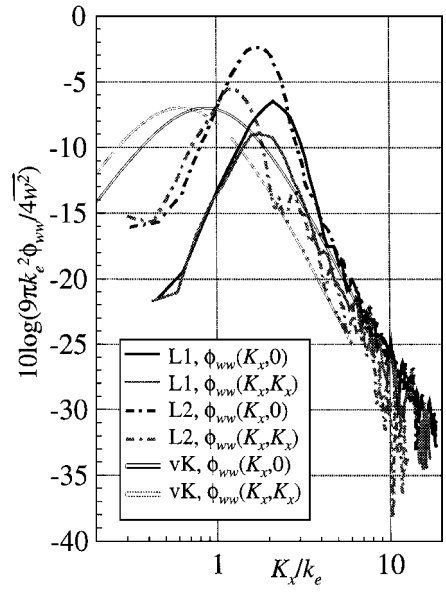

Fig. 9 Plots of $\phi_{ww}(K_x, 0)$ and $\phi_{ww}(K_x, K_x)$ for locations A/L1 and B/L2 and for the von Kármán spectrum; at location A, $k_e c = 9.0$, and at location B, $k_e c = 12.4$.

where $\kappa = K_x M/\beta^2$ and $\kappa_e^2 = \kappa^2 - k_y^2/\beta^2$. The function $\mathcal{L}$ defined in Eq. (10) is then obtained by noting that the limits of the integral can be extended to plus and minus infinity because $\Delta P = 0$ when x' is less than zero. Thus,

$$\mathcal{L}(x, K_x, k_y) = \frac{1}{i\pi\beta(\kappa_e + \kappa M + K_x)^{\frac{1}{2}}(\kappa_e - \kappa M + \gamma)^{\frac{1}{2}}} \tag{12}$$

evaluated with $\gamma = \omega(M - x/\sigma)/c_0\beta^2$. Substituting the spanwise wave number required in Eq. (8), we obtain

$$\mathcal{L}(x, K_x, k_y) = \frac{\beta}{i\pi K_x M^{\frac{1}{2}}(1 + M\cos\theta)^{\frac{1}{2}}(\cos\theta - x/\sigma)^{\frac{1}{2}}} \tag{13}$$

where $\sin\theta = y\beta/\sigma$.

By substituting Eq. (13) and the measured or von Kármán spectrum into Eq. (8), the directionality of the radiated sound field can now be evaluated, accounting for the three-dimensional blade response function. However, it is common practice in the analysis of broadband noise from flow over airfoils to use two-dimensional strip theory. In two-dimensional strip theory the blade response at each spanwise station is assumed to be the same regardless of the incoming spanwise wave number. This is equivalent to assuming that $\kappa_e = \kappa$ in Eq. (12) or $y = 0$ in Eq. (8). Therefore, we also evaluate the directionality using this approximation even though it introduces significant error.

Figure 10 compares the directionality of the acoustic field given by Eq. (8) in the $x = 0$ plane using the measured turbulence spectra and the von Kármán spectrum for both the two- and three-dimensional theories. Results are shown for a hypothetical flow Mach number of 0.7 for two different values of frequency K_x. At the lower frequency ($K_x/k_e = 1.5$, $K_x c \approx 15$; Fig. 10a), the three-dimensional theory applied either with the von Kármán or the measured spectra predicts significantly less directionality than the two-dimensional theory. Comparing the three-dimensional results, we see significantly less directionality when S_{pp} is computed with the measured spectra than when the von Kármán spectrum is used. The reason for this difference becomes apparent when Figs. 5c and 6a and Fig. 7 are compared. The wake spectra have a less rapid variation with k_y than the von Kármán spectrum because of the anisotropy of the wake turbulence. What directionality there is with the measured spectrum is almost entirely due to the three-dimensional blade response function and dipole directivity. The higher frequency example ($K_x/k_e = 6$, $K_x c \approx 65$; Fig. 10b) shows a similar result. Here for the von Kármán model, the effects of the three-dimensional blade response function and the effects of the spectrum on the directionality combine so that the three-dimensional theory agrees with the

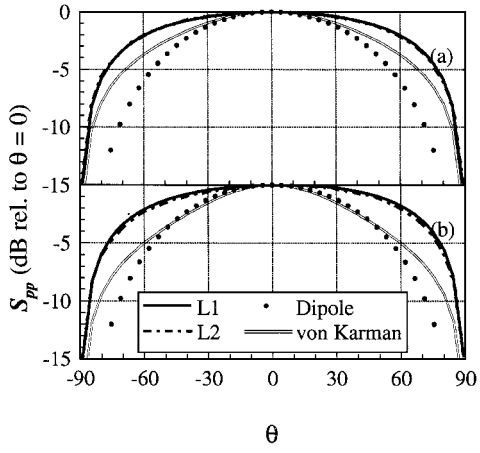

Fig. 10 Comparison of directivity calculated using the three-dimensional blade response function and L1, L2, and von Kármán spectra, with the dipole directivity given by two-dimensional strip theory at a) $K_x/k_e = 1.5$ and b) $K_x/k_e = 6.0$.

two-dimensional theory at angles of less than 50 deg. However, this does not happen for the measured spectra where the directionality is still largely produced by the three-dimensional blade response function and dipole directivity. Around this frequency the measured spectra (Figs. 5c and 6a) are almost constant with k_y for values much less than K_x and, thus, the spectral values used in the computation of S_{pp} are barely influenced by the variation of the spanwise wave number.

Therefore, we conclude that for the measured spectra Amiet's[11] approximation is valid and that $\Phi_{ww}(K_x, k_y)$ may replaced by $\Phi_{ww}(K_x, 0)$. This approximation, equivalent to assuming that the spanwise scale of the turbulence is very much less than the acoustic wavelength for all frequencies, implies an important simplification to broadband noise methodology, because directionality in the spanwise plane is determined purely by the three-dimensional blade response function.

VIII. Conclusions

Two-point velocity measurements, performed with a movable probe at varying spanwise separations relative to a fixed probe, were made in the wake of a rectangular NACA 0012 half-wing at a 5-deg angle of attack. Such profiles were measured at four locations, in the near two-dimensional part of the wake, in the stretched region where the wake begins to wind around the vortex, directly above the vortex core, and radially from the core center. For each profile, wave number frequency spectra about the location of the fixed probe were calculated.

Dominated by the large-scale organized motions present in the wake, the spectra show little similarity with the von Kármán isotropic turbulence model. Outside the core, the upwash spectra contain a single maximum at the passage frequency of these large structures. The motions associated with this peak are highly anisotropic both in terms of velocity components (wave number frequency spectra of different components being quite unalike) and in terms of length scales (all of the spectra appear stretched to varying degrees indicating that the spanwise length scale of the turbulent eddies is lower than the streamwise length scale). Opposite from what one might expect, the differences in scales do not disappear at higher wave numbers, suggesting either that the smaller scale turbulent motions are organized by the anisotropy of the large eddies or that the nonsinusoidal components of those eddies contribute significantly to the spectrum at higher wave numbers. The form of the spectra also suggests that the large eddies may to some extent modulate the smaller scale motions.

The implications of these results for broadband noise prediction have been assessed by considering the sound radiation from turbulent flow over a semi-infinite flat plate. It has been shown that the directionality in the spanwise direction is influenced by both the blade response function and the spanwise variation of the flow. The major conclusion, however, is that the correlation length scales of the flow are small compared to the acoustic wavelength and so are well represented by their values at zero spanwise wave number. However, the blade response function has a variation with spanwise wave number that cannot be ignored and significantly influences the spanwise directionality.

Acknowledgments

The authors would like to thank the Office of Naval Research, in particular L. Patrick Purtell, for their support under Grants N00014-94-1-0744 and N00014-96-1-0970 and NASA Langley Research Center, in particular Thomas Brooks and Casey Burley, for their support under Grant NAG-1-1539.

References

[1] Miranda, J. A., and Devenport, W. J., "Two Point Measurements in Trailing Vortices," AIAA Paper 96-0804, Jan. 1996.

[2] Miranda, J. A., and Devenport, W. J., "Turbulence Structure in the Spiral Wake Shed by a Lifting Wing," *AIAA Journal*, Vol. 36, No. 4, 1998, pp. 658–660.

[3] Wygnanski, I., Champagne, F., and Marasli, B., "On the Large Scale Structures in Two-Dimensional Small-Deficit Turbulent Wakes," *Journal of Fluid Mechanics*, Vol. 168, 1986, pp. 31–71.

[4] Townsend, A. A., *The Structure of Turbulent Shear Flow*, Cambridge Univ. Press, London, 1956, pp. 131–170.

[5] Antonia, R. A., and Britz, D., "Phase-Averaging in the Turbulent Far Wake," *Experiments in Fluids*, Vol. 7, No. 1, 1989, pp. 138–142.

[6] Keffer, J. F., "The Uniform Distortion of a Turbulent Wake," *Journal of Fluid Mechanics*, Vol. 22, 1965, pp. 135–159.

[7] Devenport, W. J., Rife, M. C., Liapis, S. I., and Follin, G. J., "The Structure and Development of a Wing-Tip Vortex," *Journal of Fluid Mechanics*, Vol. 312, 1996, pp. 67–106.

[8] Wittmer, K. S., "Turbulent Flowfield Downstream of a Perpendicular Airfoil–Vortex Interaction," Ph.D. Thesis, Dept. of Aerospace and Ocean Engineering, Virginia Polytechnic Inst. and State Univ., Blacksburg, VA, Oct. 1996.

[9] Wittmer, K. S., Devenport, W. J., and Zsoldos, J. S., "A Four-Sensor Hot-Wire Probe System for Three-Component Velocity Measurement," *Experiments in Fluids* (to be published).

[10] Miranda, J. A., "The Structure of a Trailing Vortex Wake," M.S. Thesis, Aerospace and Ocean Engineering Dept., Virginia Polytechnic Inst. and State Univ., Blacksburg, VA, May 1996.

[11] Amiet, R. K., "Acoustic Radiation from an Airfoil in a Turbulent Stream," *Journal of Sound and Vibration*, Vol. 41, No. 4, 1975, pp. 407–420.

[12] Barsoum, M. L., Kawall, J. G., and Keffer, J. F., "Spanwise Structure of the Plane Turbulent Wake," *Physics of Fluids*, Vol. 21, Feb. 1978, pp. 157–161.

R. W. Wlezien
Associate Editor